Research Paper
Computational Methods for Differential Equations
http://cmde.tabrizu.ac.ir
Vol. *, No. *, *, pp. 1-18
DOI:10.22034/cmde.2025.65293.2993

Thermal analysis in transformer oil-based MHD two-phase flow of Prandtl fluid through inclined channel

Mubbashar Nazeer[1], **Farooq Hussain**[2], **and Talha Anwar**[3,*]

[1]Department of Mathematics, Institute of Arts and Sciences, Government College University Faisalabad Chiniot Campus, 35400, Pakistan.

[2]Department of Mathematical Sciences (FBS) BUITEMS, Quetta 87300, Pakistan.

[3]School of Science, Walailak University, Nakhon Si Thammarat 80160, Thailand.

Abstract

This research is conducted to investigate the thermal analysis of the magneto two-phase flow of Prandtl fluid with the suspension of silver and hafnium nanoparticles through inclined walls of the channel. The momentum equations are modified under the addition of body forces to consider the impact of magnetic and gravitational forces. The heat equation is also updated with the addition of the heat flux term to capture the thermal radiation effects. The two-phase model is developed in terms of continuity, momentum, and heat equations of fluid and particle phases and uses dimensionless variables to simplify the system of equations. The dimensionless form of equations is solved by using the regular perturbation method in which the second Prandtl fluid parameter (B) is taken as a perturbation parameter and produces the analytical solution in MATHEMATICA program. The graphical results revealed many physical aspects under the physical parameters in which the first and second Prandtl fluid parameters diminish the fluid and particle phase velocity distribution. The suspension of hafnium particles in the base fluid provides more heat to the system as compared to silver nanoparticles. The particle phase velocity distribution is much greater than the fluid phase against all parameters of the study. The magnetic force has an inverse relation with the velocity and thermal profiles of both phases. The current study will help to optimize the industrial thermal management process and to design efficient cooling systems in electronic devices, and in polymer and food processing.

Keywords. Mhd two phase flow, Non-Newtonian fluid, Nano particles, Heat transfer, Transformer oil.

2010 Mathematics Subject Classification. 76A05, 76T10, 35Q79, 76D05, 65K05, 76Bxx.

1. Introduction

The non-Newtonian fluids are classified according to their behavior and shear thinning or pseudoplastic fluids are very important branches of these fluids. The apparent viscosity is diminishing under applied shear stress in these fluids. Various fluid models were proposed by researchers to examine the pseudoplastic properties of the fluids and the Prandtl fluid model is one of them (Mirza et al. [18], Riaz et al. [29]). The application of the Prandtl fluid model through asymmetric channels was presented by Akbar et al. [3] by using the numerical and perturbation methods. The mathematical model of the peristaltic flow of Prandtl fluid through stenosed arteries with permeable walls by choosing the cylindrical coordinates system has been developed by Ellahi et al. [12]. They used the mild stenosed assumption to convert the problem into simple form and applied the perturbation method to calculate the analytical solution of the problem. They observed the reduction of bolus size against the magnitude of Darcy's number. The finite element-based study of Prandtl fluid flow with the suspension of hybrid nanoparticles was conducted by Salmi et al. [32] and concluded that hybrid nanofluid produces greater heat as compared to nanofluid due to joule heating effects. Awais et al. [9] structured the mathematical model of the Prandtl fluid model towards a tilted non-rigid cylinder and obtained the solution by using the Cash and Carp numerical scheme. Their computational results revealed that the velocity

Received: 03 January 2025 ; Accepted: 08 August 2025.
∗ Corresponding author. Email: anwartalha80@gmail.com.

distribution is decreasing against the Prandtl fluid parameter. Recently, an important study of the Prandtl fluid model through ciliated walls of the channel was conducted by Sadaf et al. [30] first they developed the mathematical model and solved it numerically by adopting the Bvp4c method. Their results revealed that the magnetic field parameter enhances the velocity distribution in the center of the channel.

Magnetohydrodynamic (MHD) or magnetofluid dynamics is the study of electrically conducting fluids in which the motion of electrically conducting liquids through the magnetic field is discussed. Examples of such fluids are salt water, plasma, and liquid metals, etc. The word magnetohydrodynamics is derived from three words such as magneto (magnetic field), hydro (liquid or fluid), and dynamic (motion) (Nazeer et al. [26, 27]). A Swedish physicist Hannes Alfvén [5] is known as the pioneer of magnetohydrodynamics. The basic concept behind magnetohydrodynamics is that it induces the currents through the moving conductive liquid which in turn generates the forces on the liquid and produces the variation in the magnetic field itself. The combination of Navier-Stokes Equations (NSEs) of fluid dynamics and Maxwell's equations of electromagnetism are used to describe magnetohydrodynamics (MHD) and these differential equations can be solved analytically or numerically. The applications of trihybrid nanoparticles in MHD flow across a flat surface have been reported by Abbas et al. [1] by employing the shooting numerical technique based on the Runge-Kutta-Fehlberg method. The impact of Hall current on MHD non-Newtonian fluid with heat transfer analysis in concentric annulus was examined by Venthan et al. [34] who used the Gauss-elimination numerical approach to solve the problem. Nadeem et al. [19] highlighted the applications of convective-radiative boundary conditions in the magneto flow of non-Newtonian fluid passing through two parallel plates. They also discuss the entropy generation and heat transfer analyses graphically. They revealed that the entropy phenomena dominate under the increment of both the Brinkman number and radiation parameter. Khan et al. [15] reported the significant applications of fractional derivatives in multiphase flow of MHD fluids through two parallel walls. The outcomes of their analysis revealed the enhancement of heat transfer rate against the Peclet number. Some important studies on fluid flow are cited in (Agarwal et al. [2], Akbarov et al. [4], Cao et al. [11]).

The two-phase flow (the flow which contains more than one phase) with non-Newtonian fluids is very important in various fields namely, biological system (drug distribution, blood flow analysis and respiratory system), food industry (blending, spray drying, emulsification), chemical engineering (mineral transport, solvent extraction, power generation, petroleum refineries, chemical reactors and condensation, etc.), aerospace engineering (effective engine and rocket propulsion). These examples help to understand the importance of multiphase flows in different environments. The possible combinations of two-phase flow are gas and liquid flows, gas and solid flows, liquid and liquid flows, gas flows, and liquid and solid flows. Various researchers discussed the multiphase flows in different non-Newtonian fluid models through different geometries. For this, Alqarni et al. [7] obtained the closed-form solution of multiphase flows in ciliated walls of the channel under the impact of the electro-osmotic analysis. Their results reported the reduction in fluid velocity and pressure rise distribution under the contribution of solid particle concentration. The applications of Hall current and electric double layer in two-phase liquid were discussed by Aslam et al. [8] by using the numerical algorithm of merging and firefly. They compared their results with existing literature and observed good agreement with each other. Almutairi et al. [6] and Saleem et al. [31] discussed the suspension of metallic particles through non-Newtonian fluid to produce the two-phase flow phenomena and presented the analytical solution to the problem. Bhatti et al. [10] discussed the non-pumping flow analysis in fluid and particle suspension models by using computational software. They concluded that the pumping rate is diminishing versus the couple stress fluid parameter.

The main objective of this research is to investigate the thermal analysis of the magneto two-phase flow of Prandtl fluid with the suspension of silver and hafnium nanoparticles through inclined walls of the channel and this topic has not been discussed before. The impact of magnetic and gravitational forces is also discussed. Two dissimilar classes of two-phase fluids, hafnium-transfer oil (Hf/OT-4) and silver-transformer oil (Ag/OT-4) are taken in this research. The two-phase model is developed in terms of continuity, momentum, and heat equations of fluid and particle phases and uses dimensionless variables to simplify the system of equations. The dimensionless form of equations is solved by using the regular perturbation method in which the second Prandtl fluid parameter (B) is taken as a perturbation parameter and produces the analytical solution. The impact of various parameters on the velocity and temperature distribution of fluid and particle phases has been discussed.

2. Mathematical formulation of multiphase flow of non-Newtonian fluid

Consider the two-dimensional two-phase flow of non-Newtonian fluid through two parallel inclined walls. The flow of Prandtl fluid is investigated by taking it as a carrier fluid and mixing solid nanoparticles to develop the two-phase model. It is assumed that both walls are equal distance from the center of the channel and the distance between the lower and upper wall is 2L i.e. the lower wall is set at $y = -L$ and the top one is at $y = L$. It is also assumed that no-slip conditions are imposed on the boundary and lower and upper walls maintained the temperature T_c and T_h, respectively. The magnetic field of the strength $\mathbf{B_0}$ is applied normally to the channel and the channel is inclined with inclination angle α. The thermal radiation and viscous dissipation effects are considered and included in the heat equation, but the effects of heat generation and Joule heating are ignored and not included in the heat equation. The flow geometry with boundary conditions is displayed in Figure 1.

The particle phase (Xiong et al. [35], Nazeer et al. [23]) is governed by

$$\frac{\partial \rho_{PP}}{\partial t} + \nabla \cdot (\rho_{PP}\mathbf{V}_{PP}) = 0, \tag{2.1}$$

$$\rho_{PP}C_\alpha \frac{d\mathbf{V}_{PP}}{dt} = -C_\alpha \nabla p - RC_\alpha(\mathbf{V}_{PP} - \mathbf{V}_{FP}), \tag{2.2}$$

$$\rho_{PP}C_{PP}\frac{dT_{PP}}{dt} = \frac{\rho_{PP}C_{PP}C_\alpha}{\sigma}(T_{FP} - T_{PP}). \tag{2.3}$$

The extra stress tensor of the Prandtl fluid model (Patel & Timol [28], Shahzad [33]) is given in the following way

$$\tau_{lm} = \left(\frac{\mu_s a \sin^{-1}\left(\frac{1}{b}\Pi\right)}{\Pi}\right)\mathbf{r}_1, \quad \Pi = \sqrt{\frac{\pi}{2}}. \tag{2.4}$$

Here, μ_s is viscosity of the suspension, a and b are called the material parameters of Prandtl fluid, $\mathbf{r}_1$ is Rivlin-Erickson and $\Pi = \text{Trace}(\mathbf{r}_1)^2$ is known as the second invariant strain tensor. Thus, by using $\mathbf{V} = (u_{FP,PP}, v_{FP,PP}, 0)$, we have

$$\Pi = \sqrt{2\left(\frac{\partial u_{FP}}{\partial x}\right)^2 + \left(\frac{\partial u_{FP}}{\partial y}\right)^2 + \left(\frac{\partial v_{FP}}{\partial y}\right)^2}. \tag{2.5}$$

By adopting the property of hyperbolic function, we have

$$\sin^{-1}\left(\frac{1}{b}\Pi\right) \cong \frac{1}{b}\Pi + \frac{1}{6}\left(\frac{1}{b}\Pi\right)^3 + \left(\frac{1}{b}\Pi\right)^5 \ll 1. \tag{2.6}$$

The scalar form of Equations (2.1)–(2.6) is given by

The fluid phase

$$\frac{\partial u_{FP}}{\partial x} + \frac{\partial v_{FP}}{\partial y} = 0, \tag{2.7}$$

$$\rho_{FP}(1-C_\alpha)\left(\frac{\partial u_{FP}}{\partial t} + u_{FP}\frac{\partial u_{FP}}{\partial x} + v_{FP}\frac{\partial u_{FP}}{\partial y}\right) = -(1-C_\alpha)\frac{\partial p}{\partial x} + \mu_s(1-C_\alpha)\left(\frac{\partial \tau_{xx}}{\partial x} + \frac{\partial \tau_{xy}}{\partial y}\right) + RC_\alpha(u_{PP} - u_{FP}) - \sigma B_0^2 u_{FP} + g\rho_{FP}\sin\alpha, \tag{2.8}$$

$$\rho_{FP}(1-C_\alpha)\left(\frac{\partial v_{FP}}{\partial t}+u_{FP}\frac{\partial v_{FP}}{\partial x}+v_{FP}\frac{\partial v_{FP}}{\partial y}\right)=-(1-C_\alpha)\frac{\partial p}{\partial y}+\mu_s(1-C_\alpha)\left(\frac{\partial \tau_{xy}}{\partial x}+\frac{\partial \tau_{yy}}{\partial y}\right) +RC_\alpha(v_{PP}-v_{FP})-g\rho_{FP}\cos\alpha, \tag{2.9}$$

$$\rho_{FP}C_{FP}\left(\frac{\partial T_{FP}}{\partial t}+u_{FP}\frac{\partial T_{FP}}{\partial x}+v_{FP}\frac{\partial T_{FP}}{\partial y}\right)=K\left(\frac{\partial^2 T_{FP}}{\partial x^2}+\frac{\partial^2 T_{FP}}{\partial y^2}\right)+\frac{\rho_{PP}C_{PP}C_\alpha}{\sigma}(T_{PP}-T_{FP}) +\mu_s\left(\frac{\partial u_{FP}}{\partial x}\tau_{xx}+\frac{\partial v_{FP}}{\partial y}\tau_{yy}+\left(\frac{\partial u_{FP}}{\partial y}+\frac{\partial v_{FP}}{\partial x}\right)\tau_{xy}\right)+\frac{16\sigma KT_\infty^3}{3k_0}\left(\frac{\partial^2 T_{FP}}{\partial x^2}+\frac{\partial^2 T_{FP}}{\partial y^2}\right), \tag{2.10}$$

The particulate phase

$$\frac{\partial u_{PP}}{\partial x}+\frac{\partial v_{PP}}{\partial y}=0, \tag{2.11}$$

$$\rho_p C_\alpha\left(\frac{\partial u_{PP}}{\partial t_0}+u_{PP}\frac{\partial u_{PP}}{\partial x}+v_{PP}\frac{\partial u_{PP}}{\partial y}\right)=-C_\alpha\frac{\partial p}{\partial x}+C_\alpha R(u_{FP}-u_{PP})+g\rho_{PP}\sin\alpha, \tag{2.12}$$

$$\rho_p C_\alpha\left(\frac{\partial v_{PP}}{\partial t_0}+u_{PP}\frac{\partial v_{PP}}{\partial x}+v_{PP}\frac{\partial v_{PP}}{\partial y}\right)=-C_\alpha\frac{\partial p}{\partial y}+C_\alpha R(v_{FP}-v_{PP})-g\rho_{PP}\cos\alpha, \tag{2.13}$$

$$\rho_{PP}C_{PP}C_\alpha\left(\frac{\partial T_{PP}}{\partial t}+u_{PP}\frac{\partial T_{PP}}{\partial x}+v_{PP}\frac{\partial T_{PP}}{\partial y}\right)=\frac{\rho_{PP}C_{PP}C_\alpha}{\sigma}(T_{FP}-T_{PP}). \tag{2.14}$$

Using the assumptions of steady and uni-directional flow i.e. $\mathbf{V}_{FP,PP}=[u_{FP,PP}(y),0,0]$, is the velocity vector in which $u_{FP,PP}$ is the velocity component in the direction of x-axis and y is perpendicular to the x–axis, and $T_{FP,PP}=T_{FP,PP}(y)$, the above equations take the following form:

$$\frac{\partial u_{FP}}{\partial x}+\frac{\partial v_{FP}}{\partial y}=0, \tag{2.15}$$

$$-(1-C_\alpha)\frac{\partial p}{\partial x}+(1-C_\alpha)\frac{\partial}{\partial y}(\tau_{xy})+C_\alpha R(u_{PP}-u_{FP})-\sigma B_0^2 u_{FP}+g\rho_{FP}\sin\alpha=0, \tag{2.16}$$

$$\frac{\partial p}{\partial y}=0, \tag{2.17}$$

$$K\left(\frac{\partial^2 T_{FP}}{\partial y^2}\right)+\frac{\rho_{PP}C_{PP}C_\alpha}{\sigma}(T_{PP}-T_{FP})+\mu_s\left(\frac{\partial u_{FP}}{\partial y}\tau_{xy}\right)+\frac{16\sigma KT_\infty^3}{3k_0}\left(\frac{\partial^2 T_{FP}}{\partial y^2}\right)=0, \tag{2.18}$$

$$-C_\alpha\frac{\partial p}{\partial x}+C_\alpha R(u_{FP}-u_{PP})+g\rho_{PP}\sin\alpha=0, \tag{2.19}$$

$$\frac{\partial p}{\partial y}=0, \tag{2.20}$$

$$T_{FP}=T_{PP}. \tag{2.21}$$

The dimensional form of boundary conditions is expressed as

$$u_{FP}(y=-L)=0, \quad u_{FP}(y=L)=0, \quad T_{FP}(y=-L)=T_c, \quad T_{FP}(y=L)=T_h. \tag{2.22}$$

To convert the present problem into dimensionless form, the following dimensionless variables are introduced:

$$\bar{x}=\frac{x}{L}, \quad \bar{y}=\frac{y}{L}, \quad \bar{u}_{FP,PP}=\frac{u_{FP,PP}}{u_0}, \quad \bar{p}=\frac{p}{\mu_s u_0 \delta}, \quad \bar{T}=\frac{T}{u_0\mu_s\delta}, \quad G=\frac{gL}{u_0^2}, \quad \theta_{FP,PP}=\frac{T_{FP,PP}-T_c}{T_h-T_c}. \tag{2.23}$$

The bars have been skipped, and the dimensionless form of the equations takes the following form:

$$\frac{\partial}{\partial y}(\tau_{xy})-\frac{M_n^2}{(1-C_\alpha)}u_{FP}+\left(\frac{h_1+h_3}{h_1h_3}\right)\frac{g\sin\alpha}{(1-C_\alpha)\,\delta^2}-\frac{1}{(1-C_\alpha)\,\delta^2}\frac{\partial p}{\partial x}=0, \tag{2.24}$$

$$\frac{\partial p}{\partial y}=0, \tag{2.25}$$

$$(1+\beta)\frac{\partial^2\theta_{FP}}{\partial y^2}+Br_n\left(\frac{\partial u_{FP}}{\partial y}\tau_{xy}\right)=0, \tag{2.26}$$

$$(u_{FP}-u_{PP})=\frac{C_\alpha h_2h_3\delta^2}{C_\alpha h_3\delta^2+\sigma}\left(\frac{\partial^2\theta_{FP}}{\partial y^2}+\frac{g\sin\omega}{\delta^2}\right), \tag{2.27}$$

$$\frac{\partial p}{\partial y}=0, \tag{2.28}$$

$$\theta_{FP}=\theta_{PP}. \tag{2.29}$$

$$\tau_{xx}=\tau_{yy}=0, \quad \text{and} \quad \tau_{xy}=\left(A+B\left(\frac{\partial u_{FP}}{\partial y}\right)^2\right)\left(\frac{\partial u_{FP}}{\partial y}\right), \tag{2.30}$$

$$\left(A+B\left(\frac{\partial u_{FP}}{\partial y}\right)^2\right)\left(\frac{\partial^2 u_{FP}}{\partial y^2}\right)-\frac{M_n^2}{(1-C_\alpha)}u_{FP}+\left(\frac{h_1+h_3}{h_1h_3}\right)\frac{g\sin\alpha}{(1-C_\alpha)\delta^2}-\frac{m}{(1-C_\alpha)\delta^2}=0, \tag{2.31}$$

$$(1+\beta)\frac{\partial^2\theta_{FP}}{\partial y^2}+Br_n\left(A\left(\frac{\partial u_{FP}}{\partial y}\right)^2+B\left(\frac{\partial u_{FP}}{\partial y}\right)^4\right)=0, \tag{2.32}$$

$$u_{FP}(y=-1)=0, \quad u_{FP}(y=1)=0, \quad \theta_{FP}(y=-1)=0, \quad \theta_{FP}(y=1)=1. \tag{2.33}$$

Where $A=\frac{b}{\mu_s g}$, $B=\frac{4u_0^2}{6(ab)^2}$ are the Prandtl fluid parameters, $m=\frac{\partial p}{\partial x}$, $\delta=\frac{u_0}{Lg}$ is called the Froude number, $M_n=B_0\sqrt{\frac{\sigma}{\mu_s}}$ is known as the Hartmann number, $Br_n=\frac{\mu_s u_0}{k(T_h-T_c)}$ is called the Brinkman number and $\beta=\frac{16\tau T_\infty^3}{3k_0}$ is called the thermal radiation parameter.

3. Perturbation method

The equations (2.31) and (2.32) are nonlinear and impossible to receive the closed-form solution. But an approximate solution (Nazeer et al. [20]) can be obtained to restrict the second Prandtl fluid parameter ($B \ll 1$) by using the regular perturbation parameter.

The approximation of velocity and thermal fields are taken in the following form.

$$u_{FP} = (B)^0 u_{FP_0} + (B)^1 u_{FP_1} + (B)^2 u_{FP_2} + o(B)^3, \tag{3.1}$$

$$\theta_{FP} = (B)^0 \theta_{FP_0} + (B)^1 \theta_{FP_1} + (B)^2 \theta_{FP_2} + o(B)^3. \tag{3.2}$$

Substituting the above approximation into equations (3.34) and (3.35) and equating the powers of the second Prandtl fluid parameter to zero, one, and two (neglecting the third and higher powers of Prandtl fluid parameter B) we get the following system of equations with boundary conditions

Zeroth-order equations (B^0):

$$A\left(\frac{d^2 u_{FP_0}}{dy^2}\right) - \frac{M_n^2}{(1-C_\alpha)} u_{FP_0} + \left(\frac{h_1+h_3}{h_1 h_3}\right)\frac{g\sin\alpha}{(1-C_\alpha)\delta^2} - \frac{m}{(1-C_\alpha)} = 0, \tag{3.3}$$

$$(1+\beta)\frac{d^2\theta_{FP_0}}{dy^2} + ABr_n\left(\frac{du_{FP_0}}{dy}\right)^2 = 0, \tag{3.4}$$

$$u_{FP_0} = 0 \text{ at } y = \pm 1, \quad \theta_{FP_0} = 0 \text{ at } y = -1, \quad \theta_{FP_0} = 1 \text{ at } y = 1. \tag{3.5}$$

Zeroth-order solution (B^0):

$$u_{FP_0} = r_1 + r_2 \cosh\left(\frac{ny}{\sqrt{A}}\right), \tag{3.6}$$

$$\theta_{FP_0} = s_1 + s_2 y + s_3 y^2 + s_4 \cosh\left(\frac{2ny}{\sqrt{A}}\right). \tag{3.7}$$

First-order equations (B^1):

$$A\left(\frac{d^2 u_{FP_1}}{dy^2}\right) - \frac{M_n^2}{(1-C_\alpha)} u_{FP_1} + \left(\frac{du_{FP_0}}{dy}\right)^2\left(\frac{d^2 u_{FP_0}}{dy^2}\right) = 0, \tag{3.8}$$

$$(1+\beta)\frac{d^2\theta_{FP_1}}{dy^2} + Br_n\left(2A\left(\frac{du_{FP_0}}{dy}\right)\left(\frac{du_{FP_1}}{dy}\right) + \left(\frac{du_{FP_0}}{dy}\right)^3\right) = 0, \tag{3.9}$$

$$u_{FP_1} = 0, \quad \theta_{FP_1} = 0 \quad \text{at } y = \pm 1. \tag{3.10}$$

First-order solution (B^1):

$$u_{FP_1} = r_3 \cosh\left(\frac{ny}{\sqrt{A}}\right) + r_4 \sinh\left(\frac{ny}{\sqrt{A}}\right) + r_5 \cosh\left(\frac{3ny}{\sqrt{A}}\right), \tag{3.11}$$

$$\theta_{FP_1} = s_5 + s_6 y^2 + s_7 \sinh\left(\frac{2ny}{\sqrt{A}}\right) + s_8 \cosh\left(\frac{2ny}{\sqrt{A}}\right) + s_9 y + s_{10} \cosh\left(\frac{4ny}{\sqrt{A}}\right). \tag{3.12}$$

Second-order system (B^2):

$$A\left(\frac{d^2u_{FP_2}}{dy^2}\right)-\frac{M_n^2}{(1-C_\alpha)}u_{FP_2}+\left(\frac{du_{FP_1}}{dy}\right)^2\left(\frac{d^2u_{FP_0}}{dy^2}\right)+2\left(\frac{du_{FP_0}}{dy}\right)\left(\frac{du_{FP_1}}{dy}\right)\left(\frac{d^2u_{FP_1}}{dy^2}\right)=0, \tag{3.13}$$

$$(1+\beta)\frac{d^2\theta_{FP_2}}{dy^2}+Br_n\left(A\left(\left(\frac{du_{FP_1}}{dy}\right)^2+2\left(\frac{du_{FP_0}}{dy}\right)\left(\frac{du_{FP_2}}{dy}\right)\right)+4\left(\frac{du_{FP_0}}{dy}\right)^2\left(\frac{du_{FP_1}}{dy}\right)\right)=0, \tag{3.14}$$

$$u_{FP_2}=0,\quad \theta_{FP_2}=0\quad \text{at } y=\pm1. \tag{3.15}$$

Second-order solution (B^2):

$$u_{FP_2}=r_6\sinh\left(\frac{ny}{\sqrt{A}}\right)+(r_7+r_8y^2)\cosh\left(\frac{ny}{\sqrt{A}}\right)+r_9\sinh\left(\frac{3ny}{\sqrt{A}}\right)+r_{10}\cosh\left(\frac{3ny}{\sqrt{A}}\right)+r_{11}\cosh\left(\frac{5ny}{\sqrt{A}}\right). \tag{3.16}$$

Final perturbation solution

The final solution to the problem is expressed in the following form

$$\begin{aligned}u_{FP}&=r_1+r_2\cosh\left(\frac{ny}{\sqrt{A}}\right)+B\left(r_3\cosh\left(\frac{ny}{\sqrt{A}}\right)+r_4\sinh\left(\frac{ny}{\sqrt{A}}\right)+r_5\cosh\left(\frac{3ny}{\sqrt{A}}\right)\right)+B^2\left(r_6\sinh\left(\frac{ny}{\sqrt{A}}\right)\right.\\&\left.+(r_7+r_8y^2)\cosh\left(\frac{ny}{\sqrt{A}}\right)+r_9\sinh\left(\frac{3ny}{\sqrt{A}}\right)+r_{10}\cosh\left(\frac{3ny}{\sqrt{A}}\right)+r_{11}\cosh\left(\frac{5ny}{\sqrt{A}}\right)\right),\end{aligned} \tag{3.17}$$

$$\begin{aligned}u_{PP}&=\left(r_1+r_2\cosh\left(\frac{ny}{\sqrt{A}}\right)+B\left(r_3\cosh\left(\frac{ny}{\sqrt{A}}\right)+r_4\sinh\left(\frac{ny}{\sqrt{A}}\right)+r_5\cosh\left(\frac{3ny}{\sqrt{A}}\right)\right)\right.\\&+B^2\left(r_6\sinh\left(\frac{ny}{\sqrt{A}}\right)+(r_7+r_8y^2)\cosh\left(\frac{ny}{\sqrt{A}}\right)+r_9\sinh\left(\frac{3ny}{\sqrt{A}}\right)\right.\\&\left.\left.+r_{10}\cosh\left(\frac{3ny}{\sqrt{A}}\right)+r_{11}\cosh\left(\frac{5ny}{\sqrt{A}}\right)\right)\right)-\left(\frac{C_\alpha h_2(h_3C_\delta)^2p-g\sin(\alpha)}{C_\alpha h_3\delta^2}\right),\end{aligned} \tag{3.18}$$

$$\begin{aligned}\theta_{FP,PP}&=s_1+s_2y+s_3y^2+s_4\cosh\left(\frac{2ny}{\sqrt{A}}\right)+B\left(s_5+s_6y^2+s_7\sinh\left(\frac{2ny}{\sqrt{A}}\right)\right.\\&\left.+s_8\cosh\left(\frac{2ny}{\sqrt{A}}\right)+s_9\cosh\left(\frac{4ny}{\sqrt{A}}\right)\right)+B^2\left(s_{10}+s_{11}y^2+s_{12}y^4+s_{13}\sinh\left(\frac{2ny}{\sqrt{A}}\right)\right.\\&\left.+(s_{14}+s_{15}y^2)\cosh\left(\frac{2ny}{\sqrt{A}}\right)+s_{16}\sinh\left(\frac{4ny}{\sqrt{A}}\right)+s_{17}\cosh\left(\frac{4ny}{\sqrt{A}}\right)+s_{18}\cosh\left(\frac{6ny}{\sqrt{A}}\right)\right),\end{aligned} \tag{3.19}$$

In the above equations, $r_i(1\le i\le 11)$, and $s_j(1\le j\le 18)$, and are the constants which are bellowed.

$$n=\frac{M_n}{(1-C_\alpha)},\quad h_1=\frac{\mu_s}{U_{PPP}},\quad h_2=\frac{\mu_s}{l^2\rho},\quad h_3=\frac{\mu_s}{U_{PPP}},\quad F=\left(\frac{h_1+h_3}{h_1h_3}\cdot\frac{g\sin[\alpha]}{(1-C_\alpha)(\delta)^2}-\frac{1}{(1-C_\alpha)}\right)m, \tag{3.20}$$

$$F=\left(\frac{h_1+h_3}{h_1h_3}\cdot\frac{g\sin[\alpha]}{(1-C_\alpha)(\delta)^2}\right)-\left(\frac{1}{(1-C_\alpha)}\right)m,$$

$$r_1 = \frac{-F\sinh[n]}{n^2 r_2},$$
$$r_2 = \frac{n^2\cosh[n] - n\sinh[n]}{n^2},$$
$$r_3 = \frac{n^2 r_5\cosh[n] - 3n^2 r_5\tanh[n]}{324A},$$
$$r_4 = \frac{n^2 r_5\cosh[n]}{324A},$$
$$r_5 = \frac{-n^2 r_2^3}{324A},$$
$$r_6 = \frac{n^2 r_2^3(7\sqrt{A}r_6 - r_7)}{128A^2},$$
$$r_7 = \frac{3n^2 r_2^3 r_3}{324A},$$
$$r_8 = \frac{3n^2 r_2^3 r_4}{324A},$$
$$r_9 = \frac{-3n^2 r_3 r_2^3\cosh[n]}{324A} + \frac{n r_2^3\sinh[n]}{84A^{5/2}} - \frac{3n r_3 r_2^3\tanh[n]}{324A},$$
$$r_{10} = \frac{3n^2 r_2^3 r_3}{324A} + \frac{n^2 r_2^3 r_4}{128A^2},$$
$$r_{11} = \frac{-5n^2 r_5 r_2^3}{324A},$$
$$s_1 = \frac{1}{2(1+\beta)}\cdot\frac{Br_n n^2 r_2^2}{4(1+\beta)} + \frac{\beta}{2(1+\beta)} + \frac{4Br_n n^2\cosh[n]}{8(1+\beta)},$$
$$s_2 = \left(\frac{1}{2(1+\beta)} + \frac{\beta}{2(1+\beta)}\right),$$
$$s_3 = \frac{Br_n n^2 r_2^2}{4(1+\beta)}.$$
$$s_4 = \left(\frac{-4Br_n n^2 r_2^2}{8(1+\beta)}\right)$$
$$s_5 = \frac{1}{128A^2(1+\beta)}Br_n r_2\Big(8n(3n^2 r_3^2 - 8A^2 n r_3 - 8A^{5/2}r_4) + 16A(-n^2 r_2^3 + 2A^2(r_3 - 3r_5))\cosh\left(\frac{2n}{\sqrt{A}}\right)$$
$$+ 4A(n^2 r_2^3 + 24A^2 r_5)\cosh\left(\frac{4n}{\sqrt{A}}\right) + 32A^3 r_3\sinh\left(\frac{2n}{\sqrt{A}}\right)\Big)$$
$$s_6 = \left(\frac{-3Br_n n^2 r_3^4}{16A^2(1+\beta)} - \frac{Br_n n^2 r_2^3 r_5}{2(1+\beta)} + \frac{\sqrt{A}Br_n n^2 r_2 r_3}{2(1+\beta)}\right)$$
$$s_7 = \frac{-4Br_n n^2 r_2^2}{4(1+\beta)}$$

$$s_8 = \frac{Br_n n^2 r_2^3}{8A(1+\beta)} + \frac{Br_n n^2 r_2^3}{4(1+\beta)} + \frac{3ABr_n n^2 r_3}{4(1+\beta)}$$

$$s_9 = \frac{-128A(1+\beta)}{16(1+\beta)}$$

$$\begin{aligned} s_{10} = {} & \frac{1}{576A^3(1+\beta)} Br_n \Big(-364(4\sqrt{A}n^2 r_3^2 r_4 + 2n^4 r_2^3(4r_3 - 9r_5)) - A^3(r_4^2 - 2r_2 r_8) \\ & + 2A^2 n^2 (6r_{10}^2 - r_4^2 - r_3(r_3 - 6r_5) - 2r_2(r_7 + r_8)) \\ & + 8A^{5/2}(3n^2 r_5 - 2r_2 r_9)\cosh\left(\frac{2n}{\sqrt{A}}\right) \\ & + n\big(24n(18An^2 r_3 r_4 - 64A^{3/2} r_4 + 18n^2 r_2^3(r_3 - r_5)) - 125A^{1/2} n(r_3 r_4 - r_5 r_7) \\ & + A^2 n^2(-6r_3^2 + r_4^2 - 54r_5^2 - 2r_2(6r_7 + r_8))\big) \\ & + 9A(\sqrt{A}n^2 r_2^2 r_3 + 2n^2 r_2^3(r_3 - 9r_5) + 4A^2 n(3r_{10} r_2 - 5r_{11} r_2 + 3r_7 r_5) \\ & + A^{5/2}(6r_7 r_5 - 2r_9))\cosh\left(\frac{4n}{\sqrt{A}}\right) \\ & + 8An(3n^2 r_2^3 + A^2(10r_{11} r_2 + 9r_5))\cosh\left(\frac{6n}{\sqrt{A}}\right) \\ & + 144An(-n^2 r_2^3 + A^2(r_3 r_4 + 3r_7 r_5 + r_2 r_6 - 3r_2 r_9))\sinh\left(\frac{2n}{\sqrt{A}}\right) \\ & + 18An(r_2 r_7 + r_6) + 64A^2(r_4 r_5 + r_2 r_9)\sinh\left(\frac{4n}{\sqrt{A}}\right)\Big) \end{aligned}$$

$$s_{11} = \frac{Br_n(-3\sqrt{A}n^2 r_3^2 + 3n^2 r_2 r_3 - r_2 r_3 + A^{1/2} n^2(r_3 r_4 + 2r_3 r_5) + A^2 n^2(10r_9 + 2r_7))}{4A^3(1+\beta)}$$

$$s_{12} = \frac{Br_n(n^2 r_2^3 - 2r_2 r_3)}{4(1+\beta)}$$

$$s_{13} = \frac{Br_n(n^2 r_2^3 - 4A^2(r_3 r_4 + r_7 r_5 - 3r_2 r_9))}{16A^3(1+\beta)}$$

$$s_{14} = \frac{Br_n(4\sqrt{A}n^2 r_3 r_4 + A^2(r_4^2 + 10r_5 r_7))}{8A^2(1+\beta)}$$

$$s_{15} = \frac{Br_n(r_2^3 + 2r_2 r_3)}{4(1+\beta)}$$

$$s_{16} = \frac{Br_n(n^2 r_2^3 + A^2(r_4 r_5 + r_2 r_9))}{324(1+\beta)}$$

$$s_{17} = \frac{Br_n(-\sqrt{A}n^2 r_3(r_3 - 9r_5) - 44An^2(3r_{10} r_2 - 5r_{11} r_2 + 3r_7 r_5) + A^{5/2}(-6r_7 r_5 + 2r_9))}{64An(1+\beta)}$$

$$s_{18} = \frac{Br_n(3n^2 r_3 r_5 + A^2(10r_{11} r_2 + 9r_5))}{72A^{1/2}(1+\beta)}$$

4. Results and discussion

In the present section, the impact of physical parameters on the velocity and temperature distribution of fluid and particle phases are reported here under the admissible range. The solution is obtained in the previous section by using the regular perturbation method by restricting the second Prandtl fluid parameter ($0 < B < 1$) and developed the analytical expression of velocity and temperature distribution of both phases. Two types of nanoparticles, namely,

Hafnium and silver are mixed in transformer oil OT-4 to produce the two-phase liquids. The thermophysical properties of nanoparticles and carrier fluid are listed in Table 1.

4.1. **Velocity distribution.** The impact of the first Prandtl fluid parameter (A) on fluid and particle phase velocity distribution are displayed in Figures 2(a) and 3(b) respectively under admissible range ($0.0 \leq A \leq 3.0$). In these figures, the dotted lines show the velocity distribution under the suspension of silver nanoparticles while continuous lines are used to display the velocity field with the suspension of Hafnium nanoparticles in the carrier fluid. From these figures, it is noted that the first Prandtl fluid parameter slows down the velocity fields of fluid and particle phase extensively. Further, it is observed in Figures 3(a) and 3(b) that the second Prandtl fluid parameter ($0.1 \leq B \leq 0.3$) increases, then the same observation in fluid and particle phase velocities are captured as discussed in Figures 2(a) and 2(b). The physical reason is that when the fluid parameters are increased then these parameters increase the density of the fluid particles and as a result the velocity field decreases. It is also noted that greater velocity is observed in the core region of the channel due to applied no-slip boundary conditions at both walls of the channel.

The computational results reported that the maximum velocity of hafnium particles is much greater than silver nanoparticles against both parameters. In this scenario, the fluid phase velocity against the first Prandtl fluid parameter for the suspension of silver and hafnium particles are $(u_{FP})_m = 0.7$ and $(u_{FP})_m = 1.68$, respectively. Similarly, against the second Prandtl fluid parameter reports the maximum fluid phase velocity is $(u_{PP})_m = 1.41$ and $(u_{PP})_m = 2.93$, respectively with the suspension of silver and Hafnium particles into carrier fluid.

The impact of Froude's number (Fr) on the fluid and particle phase velocity fields are illustrated in Figures 4(a) and 4(b), respectively. Three types of flows are available in the literature based on the values of the Froude number which are critical flow, supercritical flow, and subcritical flow. A flow is said to be critical flow if the Froude number is equal to one while if the value of the Froude number is greater than one this flow is called the supercritical flow, and the subcritical flow happens when the values of the Froude number are less than one. In the current analysis, we consider the supercritical flow in which we choose the values of Froude number greater than one. It is observed from Figures 4 that the velocity of both phases is retarded against the values of Froude number. Again, the particle phase velocity field is much greater than the velocity field of the fluid phase, and a greater magnitude of velocity is observed at the center region of the channel.

Figures 5(a) and 5(b) are displayed to see the impact of Hartman number on the velocity distribution of fluid and particle phases. From these graphs, it is evident that the Hartman number decreases the velocity distribution. As expected, the magnetic field resists the flow field. It is also seen that the velocity profiles of silver nanoparticles are much less than the suspensions of Hafnium particles through regular Figures 6(a) and 6(b) depict the variation of velocities for different angles of inclination. To construct these figures, we used the values of inclination as selected. These figures elaborated that the velocity fields strongly depend on the angle of inclination which shows the increasing trend with this parameter. The physical reason is that when the channel is more inclined the effects of gravitation increase which helps to increase the motion of the fluid particle as a result the velocity fields are increased significantly. The impact of constant pressure gradient on the fluid and particle phases velocities are constructed in Figures 7(a) and 7(b). It was observed that the pressure gradient parameter promotes the velocity fields. The reason is that when more pressure is applied on the fluid then greater motion is produced in fluid particles which causes the development in the velocity field.

4.2. **Temperature fields.** The behavior of the fluid and particle phase thermal profiles against the first and second Prandtl fluid parameters is plotted in Figures 8(a) and 8(b), respectively. From these figures, it is observed that the first fluid parameter diminishes the thermal profile, while the second fluid parameter enhances it. It is also noted that the temperature reaches a minimum at $y = 0$ due to the applied boundary conditions. $(\theta_{F,P})_{(y=0)} = 0$, i.e. the lower wall is cold. Further, the temperature of hafnium particles provides more temperature profiles as compared to silver nanoparticles due to the greater density of the hafnium particles. Figures 9(a) and 9(b) illustrate how the angle of inclination and volume fraction density of the hafnium and silver nanoparticles affect the temperature distribution of both phases.

It is perceived that both parameters developed the temperature profiles when they are increased under the acceptable range. The physical reason is that when the number of nanoparticles of hafnium and silver increase then they

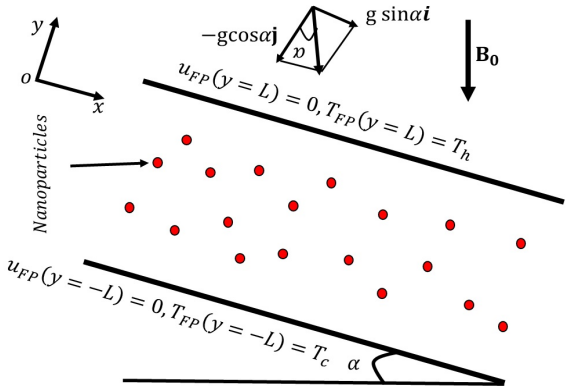

FIGURE 1. Flow configuration.

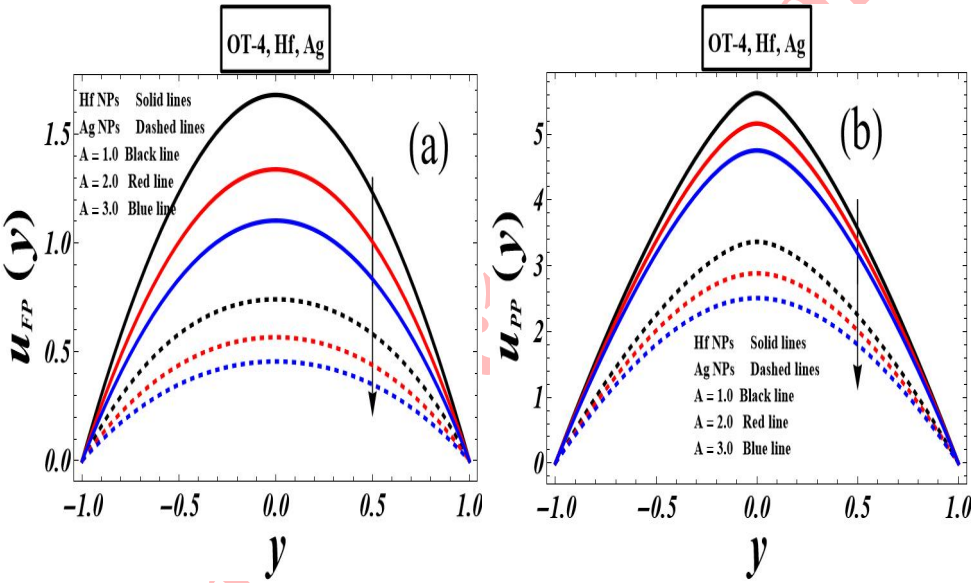

FIGURE 2. Impact of first Prandtl fluid parameter on fluid phase (a) and particulate phase (b) velocity.

generate more heat during the suspension in base fluid which causes the temperature profile to increase against the volume fraction density of the particles. The impact of the Hartman number and thermal radiation parameter on the temperature distribution is recorded in Figure 10(a) and 10(b), respectively, and it is noted that the Hartman number and thermal radiation parameter both have an inverse relation with temperature distribution which means that when Hartmann number or thermal radiation parameter increases then the profile of temperature decreases significantly. The influence of the Brinkman number and pressure gradient parameter on the temperature field is shown in Figures 11(a) and 11(b), respectively. Both figures indicate the increasing behavior of the Brinkman number and pressure gradient parameter with temperature distribution. The physical reason is that when the Brinkman number is increased then more thermal energy is entering into the system, and the temperature field increases versus the Brinkman number. Furthermore, when more pressure is applied to the fluid then the collisions in the particles increase which causes the enhancement in the temperature profile.

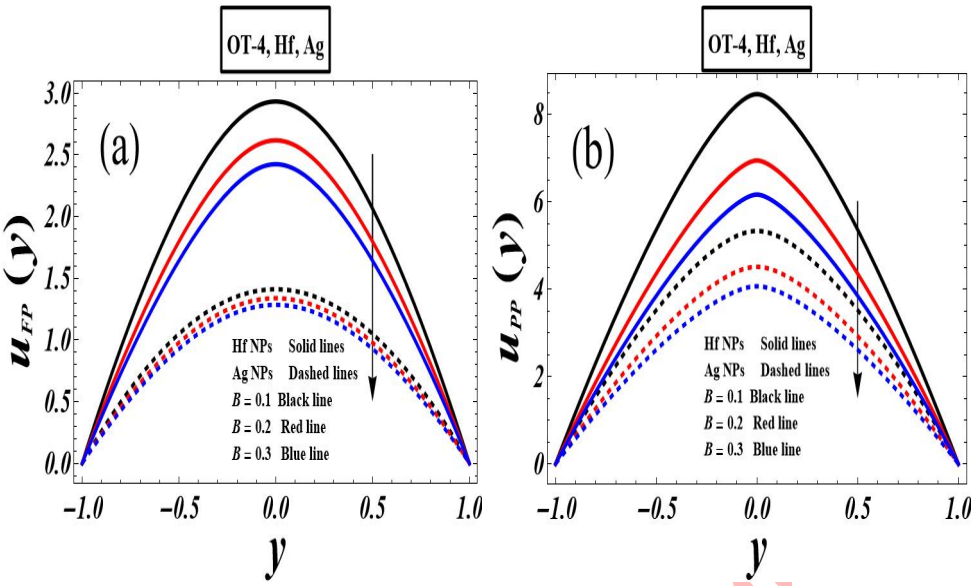

FIGURE 3. Impact of second Prandtl fluid parameter on fluid phase (a) and particulate phase (b) velocity.

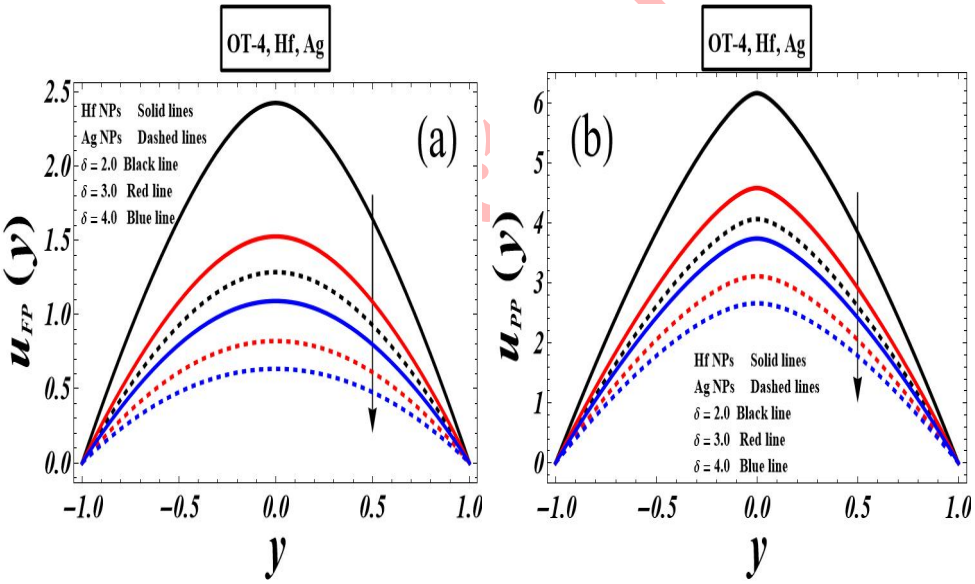

FIGURE 4. Impact of Froude number on fluid phase (a) and particulate phase (b) velocity.

TABLE 1. Physical properties of base fluid and nanoparticles.

	$Viscosity(300K)$	$Density(Kg/m^3)(300K)$	$Reference$
Transformer Oil (OT-4)	13.73×10^{-3} Pas	837 Kgm^{-3}	Lee et al. [16, 17]
Silver (Ag)	–	10500 Kgm^{-3}	Irfan et al. [14], Nazeer et al. [25]
Hafnium (Hf)	–	13310 Kgm^{-3}	Nazeer et al. [21, 22]

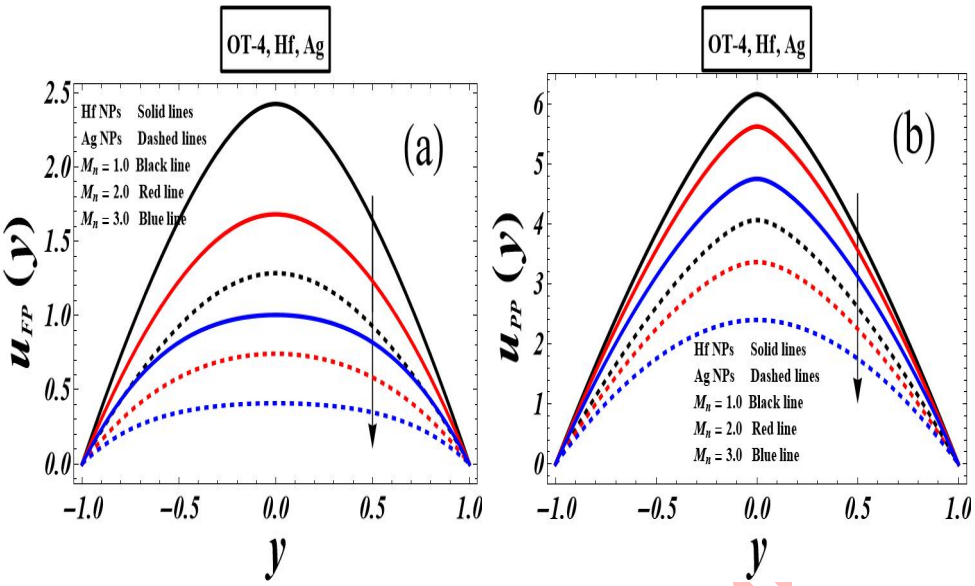

FIGURE 5. Impact of Hartman number on fluid phase (a) and particulate phase (b) velocity.

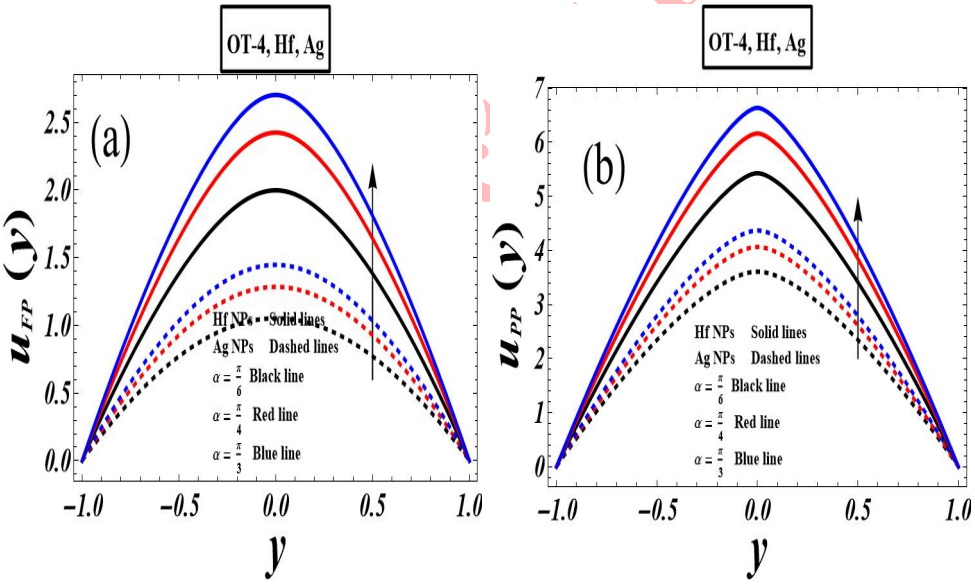

FIGURE 6. Impact of inclination angle on fluid phase (a) and particulate phase (b) velocity.

5. CONCLUSION

This study is conducted to investigate the thermal analysis of the two-phase flow of Prandtl fluid suspended by silver and hafnium nanoparticles under the impact of thermal radiation, magnetic field, and gravitational force through inclined parallel plates. By using the dimensionless parameters, the problem is transformed into a dimensionless form and solved by using the regular perturbation method which produces the analytical solution of velocity and temperature distribution. The key results of the comprehensive examinations are given as follows.

i. The Prandtl fluid parameters decline the velocity of both phases.
ii. The magnetic force produces a decline in behavior in velocity and temperature fields.
iii. More nanoparticles in the base fluid develop the temperature distribution.
iv. The velocity and temperature of both phases are greater under the suspension of hafnium particles as compared to silver.

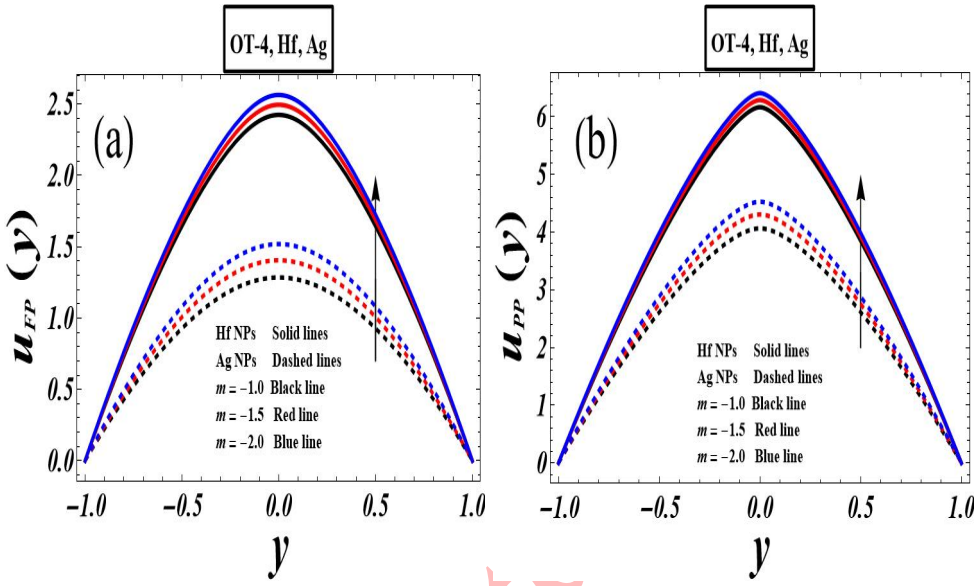

FIGURE 7. Impact of pressure gradient on fluid phase (a) and particulate phase (b) velocity.

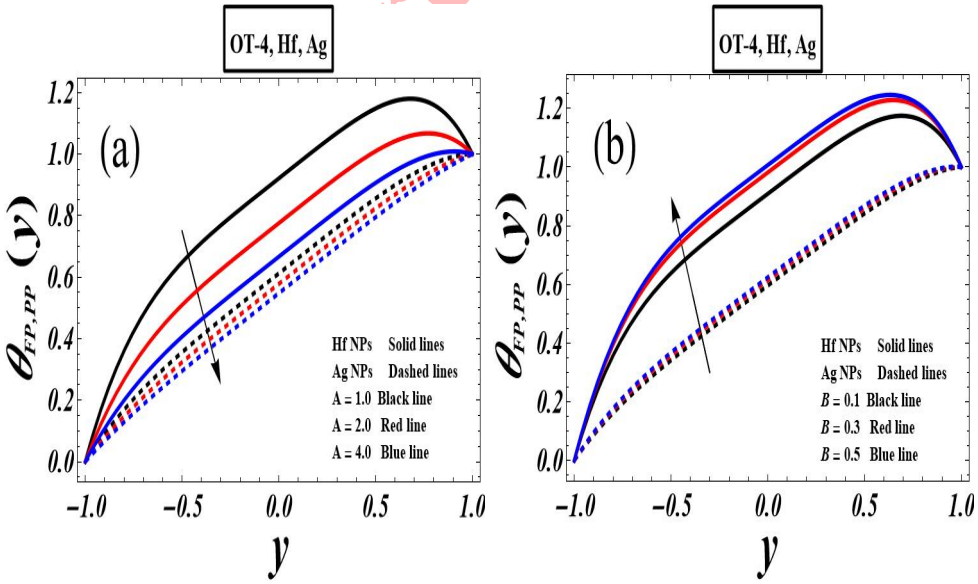

FIGURE 8. Impact of first Prandtl fluid parameter (a) and second Prandtl fluid parameter (b) on thermal profile.

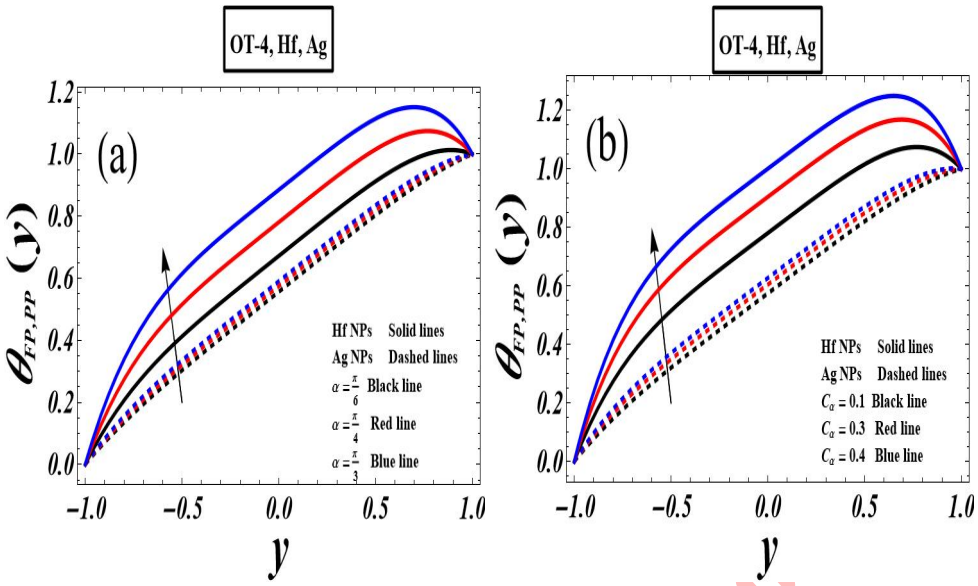

FIGURE 9. Impact of angle of inclination (a) and density number (b) on thermal profile.

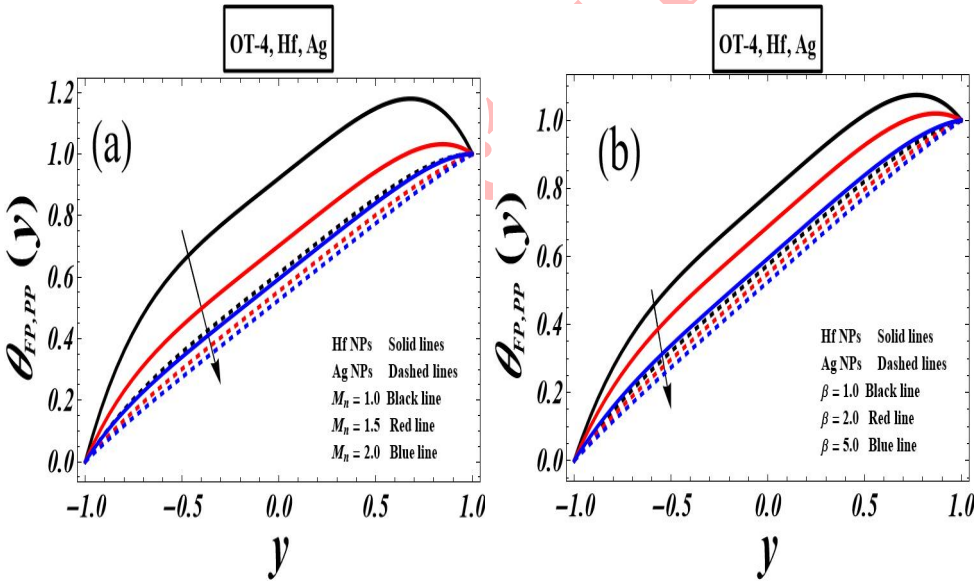

FIGURE 10. Impact of magnetic field parameter (a) and thermal radiation parameter (b) on thermal profile.

v. The particle phase velocity distribution is much greater than the fluid phase velocity against all physical parameters.
vi. The first Prandtl fluid parameter enhances the temperature while the second Prandtl fluid parameter declines the temperature distribution.

Conflict of interest: The authors have no conflict of interest related to this research.
Funding: No funding is received against this research.

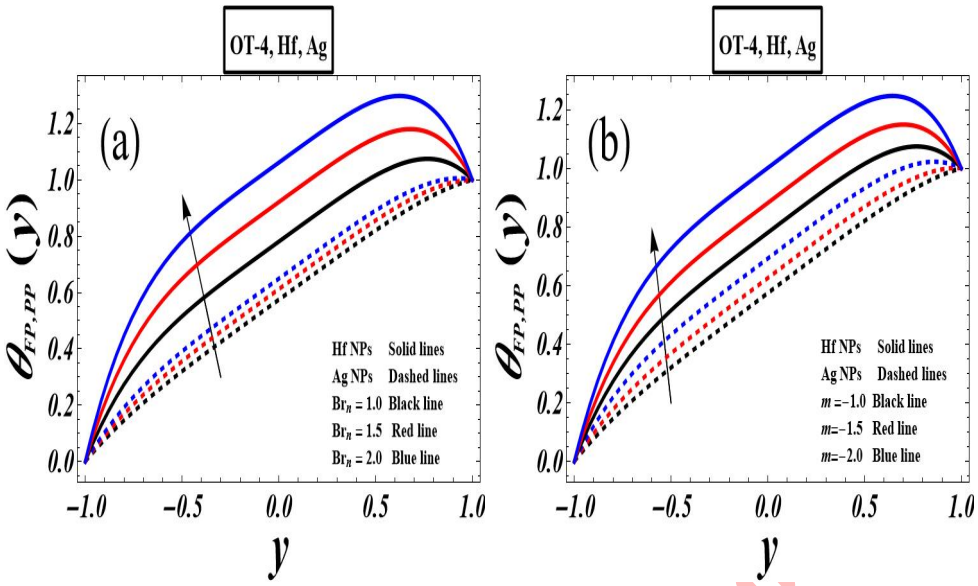

FIGURE 11. Impact of Brinkman number (a) and pressure gradient parameter (b) on thermal profile.

Data Availability Statement All the data is available in the manuscript.
Credit Author statement:
Mubbashar Nazeer: Software; Supervision, Roles/Writing – original draft; Writing – review & editing.
Farooq Hussain: Investigation; Methodology, Visualization.
Talha Anwar: Formal analysis, Writing-review & editing.

REFERENCES

[1] M. Abbas, N. Khan, M. S. Hashmi, R. K. Alhefthi, S. Rezapour, and M. Inc, *Thermal Marangoni convection in two-phase quadratic convective flow of dusty MHD trihybrid nanofluid with non-linear heat source*. Case Studies in Thermal Engineering, *57*(1) (2024), 104190.
[2] R. P. Agarwal, A. M. Alghamdi, S. Gala, and M. A. Ragusa, *On the regularity for weak solutions to the micropolar fluid flows*. Applied and Computational Mathematics,*23*(4) (2024), 558-569.
[3] N. S. Akbar, S. Nadeem, and C. Lee, *Peristaltic flow of a Prandtl fluid model in an asymmetric channel*. International Journal of Physical Sciences,*7*(5) (2012), 687-695.
[4] S.D Akbarov, G. J. Valiyev, S. A. Aliyev, and Z. F. Khankishiyev,*The influence of the inhomogeneous initial stresses in the hollow cylinder containing an inviscid fluid on the dispersion of the quasi-Scholte waves propagating in this cylinder*. Applied and Computational Mathematics, *23*(1) (2024), 18-39.
[5] H. Alfvén, *Existence of electromagnetic-hydrodynamic waves*. Nature, *150*(3805) (1942) 405-406.
[6] S. Almutairi, F. Hussain, M. Nazeer, S. Saleem, and R. S. Mohammed, *Perturbation solution of multiphase flow of Williamson fluid through convergent and divergent conduits: Electro-osmotic effects*. Modern Physics Letters B, *38*(34) (2024), 2450348.
[7] M. M. Alqarni, A. Riaz, M. Shehzadi, G. Alhamzi, and E. E. Mahmoud, *A multiphase ciliary flow of Casson fluid in a porous channel under the effects of electroosmosis and MHD: Exact solutions*. Results in Physics, *52* (2023), 106947.
[8] M. N. Aslam, A. Riaz, N. Shaukat, M. W. Aslam, and G. Alhamzi, *Machine learning analysis of heat transfer and electroosmotic effects on multiphase wavy flow: A numerical approach*. International Journal of Numerical Methods for Heat & Fluid Flow, *34*(1)(2024), 150-177.

[9] M. Awais, S. Bilal, K. Ur Rehman, and M. Y. Malik, *Numerical investigation of MHD Prandtl melted fluid flow towards a cylindrical surface: comprehensive outcomes*. Canadian Journal of Physics,*98*(3)(2020), 223-232.

[10] M. M. Bhatti, A. Zeeshan, M. A. Asif, R. Ellahi, and S. M. Sait, *Non-uniform pumping flow model for the couple stress particle-fluid under magnetic effects*. Chemical Engineering Communications, *209*(8) (2022), 1058-1069.

[11] W. Cao, S. U. Rehman, M. I. Asjad, and M. Inc, *Numerical study of bioconvection and Cattaneo-Christov heat flux model in MHD Maxwell nanofluid flow over a variable thickness elastic surface*. Applied and Computational Mathematics, *23*(2) (2024), 182-200.

[12] R. Ellahi, S. U. Rahman, S. Nadeem, and K. Vafai, *The blood flow of Prandtl fluid through a tapered stenosed arteries in permeable walls with magnetic field*. Communications in Theoretical Physics, *63*(3) (2015), 353.

[13] F. Hussain, M. Nazeer, M. Altanji, A. Saleem, and M. M. Ghafar, *Thermal analysis of Casson rheological fluid with gold nanoparticles under the impact of gravitational and magnetic forces*. Case Studies in Thermal Engineering, *28*(2021), 101433.

[14] M. Irfan, I. Siddique, M. Nazeer, and W. Ali, *Theoretical study of silver nanoparticle suspension in electroosmosis flow through a nonuniform divergent channel with compliant walls: a therapeutic application*. Alexandria Engineering Journal,*86* (2024), 443-457.

[15] D. Khan, S. Ullah, P. Kumam, W. Watthayu, Z. Ullah, and A. M. Galal, *A generalized dusty Brinkman type fluid of MHD free convection two phase flow between parallel plates*. Physics Letters A, *450* (2022), 128368.

[16] J. C. Lee, and W. Y. Kim, *Experimental study on the dielectric breakdown voltage of the insulating oil mixed with magnetic nanoparticles*. Physics Procedia, *32*(2012), 327-334.

[17] J. C. Lee, H. S. Seo, and Y. J. Kim, *The increased dielectric breakdown voltage of transformer oil-based nanofluids by an external magnetic field*. International Journal of Thermal Sciences, *62*(2012), 29-33.

[18] C. R. Mirza, M. Nazeer, M. R. Hamoudi, G. Rasool, N. B. Khedher, S. A. Abdelmohsen, and R. Ghodhbani, *Performance evaluation of flow and thermal behavior in two-phase Prandtl fluid using perturbation analysis*. International Communications in Heat and Mass Transfer, *167*(2025), 109246.

[19] S. Nadeem, B. Ishtiaq, J. Alzabut, and H. A. Ghazwani, *Entropy generation for exact irreversibility analysis in the MHD channel flow of Williamson fluid with combined convective-radiative boundary conditions*. Heliyon, *10*(4)(2024), e26432

[20] M.Nazeer, N. Ali, F. Ahmad, W. Ali, A.Saleem, Z. Ali, and A. Sarfraz, *Effects of radiative heat flux and joule heating on electro-osmotically flow of non-Newtonian fluid: analytical approach*. International Communications in Heat and Mass Transfer, *117*(2020), 104744.

[21] M. Nazeer, F. Hussain, M. M. Ghafar, and M. A. Javed, *Investigation of electro-osmotic flow of Hafnium particles mixed-up with Casson fluid in convergent geometry: Theoretical study of multiphase flow*. Partial Differential Equations in Applied Mathematics, *6* (2022), 100448.

[22] M. Nazeer, F. Hussain, M. I. Khan, Q. Shahzad, Y. M. Chu, and S. Kadry, *MHD two-phase flow of Jeffrey fluid suspended with hafnium and crystal particles: analytical treatment*. Numerical Methods for Partial Differential Equations, *40*(2) (2024), e22766.

[23] M. Nazeer, F. Hussain, Q. Shahzad, M. I. Khan, S. Kadry, and Y. M. Chu, *Perturbation solution of the multiphase flows of third grade dispersions suspended with Hafnium and crystal particles*. Surfaces and Interfaces,*22*(2021), 100803.

[24] M. Nazeer, F. Hussain, M. Türkyılmazoğlu, and Z. Ali, *Towards an approximate solution of highly viscous electro-osmotic flows in inclined Channel: Applications in petroleum and gas engineering*. Journal of Magnetism and Magnetic Materials, *577*(2023), 170793.

[25] M. Nazeer, K. Ramesh, H. Farooq, and Q. Shahzad, *Impact of gold and silver nanoparticles in highly viscous flows with different body forces*. International Journal of Modelling and Simulation, *43*(4)(2023), 376-392.

[26] M. Nazeer, S. Saleem, and M. W. Nazir, *Controlling the convective heat transfer of shear thinning and shear thickening fluids in parallel plates with magnetic force*. Zeitschrift für Naturforschung A, *80*(6)(2025), 469-483.

[27] M. Nazeer, S. Salatima, M. Imran, and N. Radwan, *Role of zeta potential and slip boundary conditions to improve the heat transfer analysis of hybrid nanofluid*. Journal of Radiation Research and Applied Sciences, *18*(3) (2025), 101702.

[28] M. Patel, and M. G. Timol, *The stress-strain relationship for visco-inelastic non-Newtonian fluids*. International Journal of Applied Mathematics and Mechanics, *6*(12)(2010), 79-93.

[29] M. B. Riaz, Saddiqa, A., and S. Bilal, *Peristaltic transport in Prandtl fluid with diffusion and activation energy aspects by executing numerical simulations*. International Communications in Heat and Mass Transfer, *163*(2025), 108742.

[30] H. Sadaf, Z. Asghar, and N. Iftikhar, *Metachronal wave impact in a channel flow of Prandtl fluid model*. International Communications in Heat and Mass Transfer, *155*(2024), 107464.

[31] S. Saleem, M. Nazeer, N. Radwan, and H. Abutuqayqah, *Significance of hafnium nanoparticles in hydromagnetic non-Newtonian fluid-particle suspension model through divergent channel with uniform heat source: thermal analysis*. Zeitschrift für Naturforschung A, *79*(6)(2024), 567-582.

[32] A. Salmi, H. A. Madkhali, B. Ali, M. Nawaz, S. O. Alharbi, and A. S. Alqahtani, *Numerical study of heat and mass transfer enhancement in Prandtl fluid MHD flow using Cattaneo-Christov heat flux theory*. Case Studies in Thermal Engineering, *33*(2022), 101949.

[33] M. H. Shahzad, A. U. Awan, S. Nadeem, N. A. Ahammad, H. Hamam, A. Alamer, and S. Shafique, *Rheological effects in peristaltic flow of Prandtl fluid through elliptical duct: A comprehensive analysis*. ZAMM-Journal of Applied Mathematics and Mechanics/Zeitschrift für Angewandte Mathematik und Mechanik,*104*(9)(2024), e202400094.

[34] S. M. Venthan, P. S. Kumar, S. S. Kumar, S. Sudarsan, and G. Rangasamy, *A computational study of the impact of fluid flow characteristics on convective heat transfer with Hall current using the MHD non-Newtonian fluid model*. Chemical Engineering Research and Design, *203*(2024), 789-799.

[35] P. Y. Xiong, M. Nazeer, F. Hussain, M. I. Khan, A. Saleem, S. Qayyum, and Y. M. Chu, *Two-phase flow of couple stress fluid thermally effected slip boundary conditions: Numerical analysis with variable liquids properties*. Alexandria Engineering Journal, *61*(5)(2022), 3821-3830.